

<https://doi.org/10.15407/ujpe66.4.341>

A.I. POGODIN,<sup>1</sup> V.I. STUDENYAK,<sup>1</sup> M.Y. FILEP,<sup>1</sup> O.P. KOKHAN,<sup>1</sup>  
I.P. STUDENYAK,<sup>1</sup> P. KÚŠ<sup>2</sup>

<sup>1</sup> Uzhhorod National University

(46, Pidhirna Str., Uzhhorod, Ukraine; e-mail: studenyak@dr.com)

<sup>2</sup> Comenius University

(Mlynska dolina, Bratislava, Slovakia)

## INFLUENCE OF CATION SUBSTITUTION ON IONIC AND ELECTRONIC CONDUCTIVITY OF $(\text{Cu}_{1-x}\text{Ag}_x)_7\text{GeS}_5\text{I}$ MIXED CRYSTALS

*Impedance measurements of  $(\text{Cu}_{1-x}\text{Ag}_x)_7\text{GeS}_5\text{I}$  mixed crystals are carried out in the frequency range from 10 Hz to 300 kHz and in the temperature interval 292–383 K. The temperature and frequency dependences of the electrical conductivity for  $(\text{Cu}_{1-x}\text{Ag}_x)_7\text{GeS}_5\text{I}$  mixed crystals are studied. Based on the analysis of Nyquist plots and using the electrode equivalent circuits, the values of ionic and electronic components of the electrical conductivity are determined. The compositional behavior of the ionic and electronic conductivities, as well as the compositional behavior of their activation energies, are discussed. The ratio of ionic and electronic components of the conductivity for  $(\text{Cu}_{1-x}\text{Ag}_x)_7\text{GeS}_5\text{I}$  mixed crystals was analyzed.*

*Keywords:* mixed crystals, electrical conductivity, Nyquist plot, activation energy, compositional dependence.

### 1. Introduction

Recently, much attention of researchers has been drawn to searching and investigating the new materials for their use in modern devices for the production, conversion, accumulation, and storage of energy [1–4]. Among such materials, a significant role is played by superionic materials with the structure of the argyrodite, which include germanium-containing compounds  $\text{Me}_7\text{GeS}_5\text{I}$  ( $\text{Me} = \text{Cu}, \text{Ag}$ ) [5, 6]. On the basis of argyrodite, new types of batteries, high-capacity capacitors, ionistors can be created, etc. The wide possibilities to substitute atoms in argyrodites allow one to conduct a purposeful search for solid-electrolytic materials with high operational parameters. At present, the influence of atomic substitution processes in cationic and anionic sublattices in phosphorus-containing argyrodites (for example, [7–9]) is well studied. In addition, much attention is paid to the production of argyrodites in the form of composites, ceramics, and thin films [10–13]. It should be noted that, in recent years, along with Li-containing argyrodites (e.g., [14–19]) K-containing argyrodites begin to be investigated [20]. The investigation of the

growth, and structural, electrical, and optical properties of Ge-containing argyrodites were carried out in [21–24]. In [25], it was established that the electrical conductivity of  $(\text{Cu}_{1-x}\text{Ag}_x)_7\text{GeS}_5\text{I}$  mixed crystals with the increase of silver content nonlinearly decreases, while the activation energy had shown the nonlinear compositional dependence and achieved a maximum for  $(\text{Cu}_{0.5}\text{Ag}_{0.5})_7\text{GeS}_5\text{I}$  mixed crystal. In [25], a good interrelation between structural and electrical properties in  $(\text{Cu}_{1-x}\text{Ag}_x)_7\text{GeS}_5\text{I}$  mixed crystals was shown. Thus, the compositional dependence of the maximal distance between the moving positions being a limiting factor for the migration of cations was in a good agreement with the compositional dependence of the activation energy. In addition, the site occupation factor for mobile atoms in mixed crystals increases, which causes a decrease of their mobility and electrical conductivity [25]. In [26], it was shown that the presence of a domain structure can influence the electrical properties of argyrodites. The nature of the domains may be associated with the presence of a mosaic crystal texture. In this case, the domain boundaries represent a structural inhomogeneity, which manifests itself in the disorientation of the texture elements  $<1^\circ$  [27]. However, a detailed analysis of the compositional behavior of electrical properties

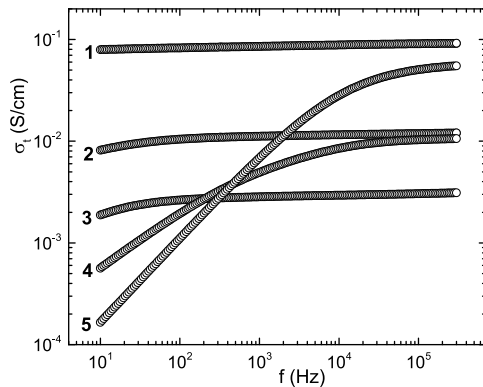


**Fig. 1.** Frequency dependences of the total electrical conductivity at  $T = 298$  K for  $(\text{Cu}_{1-x}\text{Ag}_x)_7\text{GeS}_5\text{I}$  mixed crystals:  $\text{Cu}_7\text{GeS}_5\text{I}$  (1),  $(\text{Cu}_{0.75}\text{Ag}_{0.25})_7\text{GeS}_5\text{I}$  (2),  $(\text{Cu}_{0.5}\text{Ag}_{0.5})_7\text{GeS}_5\text{I}$  (3),  $(\text{Cu}_{0.25}\text{Ag}_{0.75})_7\text{GeS}_5\text{I}$  (4), and  $\text{Ag}_7\text{GeS}_5\text{I}$  (5)

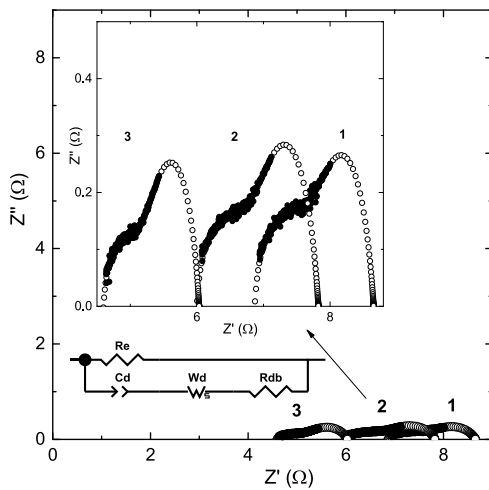


**Fig. 2.** Nyquist plots for  $\text{Cu}_7\text{GeS}_5\text{I}$  crystal at 298 K (1), 323 K (2), and 373 K (3): experimental data (solid symbols), modeled (calculated) data (open symbols), and EEC

of  $(\text{Cu}_{1-x}\text{Ag}_x)_7\text{GeS}_5\text{I}$  mixed crystals, namely ionic and electronic components of the electrical conductivity and their activation energies has not been carried out so far. Thus, the aim of this paper is to investigate the influence of the cation substitution on ionic and electronic conductivities, as well as on their activation energies for  $(\text{Cu}_{1-x}\text{Ag}_x)_7\text{GeS}_5\text{I}$  mixed crystals.

## 2. Experimental

$(\text{Cu}_{1-x}\text{Ag}_x)_7\text{GeS}_5\text{I}$  mixed crystals were grown by the vertical zone crystallization method described in [25]. The identification of the above-mentioned compounds was carried out with powder method using the diffraction patterns measured by a DRON 4-07

diffractometer (conventional  $\theta - 2\theta$  scanning method, Bragg angle  $2\theta \cong 10 - 60^\circ$ , Ni-filtered  $\text{CuK}\alpha$  radiation). The diffractograms of  $(\text{Cu}_{1-x}\text{Ag}_x)_7\text{GeS}_5\text{I}$  compounds were indexed as a face-centered cubic cell with the space group F-43m, the number of formula units per unit cell  $Z = 4$ . Investigation of the electrical conductivity of  $\text{Cu}_7\text{GeS}_5\text{I}$  and  $\text{Ag}_7\text{GeS}_5\text{I}$  crystals, as well as for  $(\text{Cu}_{1-x}\text{Ag}_x)_7\text{GeS}_5\text{I}$  mixed crystals with  $x = 0.25, 0.5, 0.75$  was carried out by impedance spectroscopy [28], in the frequency range from 10 Hz to 300 kHz and the temperature interval 292–383 K using a high-precision LCR meter AT-2818. The amplitude of the alternating current constituted 10 mV. The measurement was carried out by the two-electrode method, on blocking (electronic) gold contacts. Gold contacts for measurements were applied by the chemical precipitation from solutions [28].

## 3. Results and Discussion

For  $\text{Cu}_7\text{GeS}_5\text{I}$  and  $\text{Ag}_7\text{GeS}_5\text{I}$  crystals, as well as for mixed crystals  $(\text{Cu}_{1-x}\text{Ag}_x)_7\text{GeS}_5\text{I}$  mixed crystals with  $x = 0.25, 0.5, 0.75$ , the measured dependences of the total conductivity on the frequency are presented in Fig. 1. It is shown that an increase in the conductivity with a frequency is observed, being characteristic of materials with ionic conductivity in the solid state [29]. For the detailed studies of the frequency behavior of the electrical conductivity and its separation into ionic and electronic components, a standard approach using electrode equivalent circuits (EEC) [30, 31], and their analysis on Nyquist plots was used. The parasitic inductance of the cell ( $\sim 2 \times 10^{-8}$  H) is taken into account during the analysis of all samples. In the studied frequency range, two semicircles are observed on the Nyquist plots for both  $\text{Cu}_7\text{GeS}_5\text{I}$  and  $\text{Ag}_7\text{GeS}_5\text{I}$  crystals, as well as for  $(\text{Cu}_{1-x}\text{Ag}_x)_7\text{GeS}_5\text{I}$  mixed crystals. During the analysis of the frequency behavior of  $\text{Cu}_7\text{GeS}_5\text{I}$  crystal in  $Z' - Z''$  coordinates, it was established that  $\sigma_{\text{ion}} \ll \sigma_{\text{el}}$ . The processes of ionic diffusion within the double diffusion layer take place in the low-frequency region, which is reflected on EEC by means of successively included elements  $W_d$  (ion diffusion) and  $C_d$  (capacity of the double diffusion layer), respectively. The resistance of the domain boundaries  $R_{db}$  is responsible for the high-frequency semicircle. Thus, the ionic conductivity of  $\text{Cu}_7\text{GeS}_5\text{I}$  crystal is determined by the sum of the diffusion resistance  $W_d - R$

and the resistance of the domain boundaries  $R_{db}$ . In parallel to the elements corresponding to the ionic processes, the electronic resistance  $R_e$  is included in the EEC. It determines the electronic component of the conductivity, and contributes to the nature of both observed semicircles (Fig. 2). It should be noted that  $(\text{Cu}_{1-x}\text{Ag}_x)_7\text{GeS}_5\text{I}$  mixed crystals with  $x = 0.25, 0.5$  are characterized by a more complex and disordered structure, which influenced the appearance of Nyquist plots, being manifested in the change of a shape and the ratio of the semicircles dimensions (Fig. 3).

This, first of all, is associated with a change in the ratio between ionic and electronic conductivities ( $\sigma_{\text{ion}} \sim \sigma_{\text{el}}$ ) with cationic  $\text{Cu}^+ \leftrightarrow \text{Ag}^+$  substitution, which is caused by structural changes in the process of mixed crystals formation. For  $(\text{Cu}_{0.75}\text{Ag}_{0.25})_7\text{GeS}_5\text{I}$  (Fig. 3, a) and  $(\text{Cu}_{0.5}\text{Ag}_{0.5})_7\text{GeS}_5\text{I}$  (Fig. 3, b) mixed crystals, the character, shape, and the ratio of the dimensions of semicircles in the Nyquist plots indicate a decrease in the electronic component of the conductivity in comparison with  $\text{Cu}_7\text{GeS}_5\text{I}$  crystal. The low-frequency semicircles in the Nyquist plots correspond to diffusion relaxation processes at the electrode/crystal boundary and the electronic conductivity displayed on the EEC by the capacity of the double diffusion layer  $C_d$  connected in parallel to the electronic resistance  $R_e$  (Fig. 3). In addition, in the process of cationic  $\text{Cu}^+ \leftrightarrow \text{Ag}^+$  substitution during the transition from  $(\text{Cu}_{0.75}\text{Ag}_{0.25})_7\text{GeS}_5\text{I}$  mixed crystal to  $(\text{Cu}_{0.5}\text{Ag}_{0.5})_7\text{GeS}_5\text{I}$  mixed crystal, there is an obvious tendency to shift the low-frequency semicircle into the low-frequency region, which may be associated with the increasing influence of diffusion ionic processes in connection with decrease of the electronic component of the conductivity and, as a result, with the increase in the time of ionic relaxation. High-frequency semicircles, in their turn, correspond to the processes of ionic conductivity at the boundaries of domains, which are reflected by the ionic resistance  $R_{db}$  with parallelly connected capacity of domain boundaries  $C_{db}$ . In parallel to the elements corresponding to the bulk ionic processes, the electronic resistance  $R_e$  is included in the EEC (Fig. 3). The ionic conductivity on EEC is determined by the resistance of domain boundaries  $R_{db}$ , and the electronic conductivity is determined by the resistance  $R_e$ . Further increase in the content of  $\text{Ag}^+$  ions during the transition from  $(\text{Cu}_{0.25}\text{Ag}_{0.75})_7\text{GeS}_5\text{I}$  mixed crystal

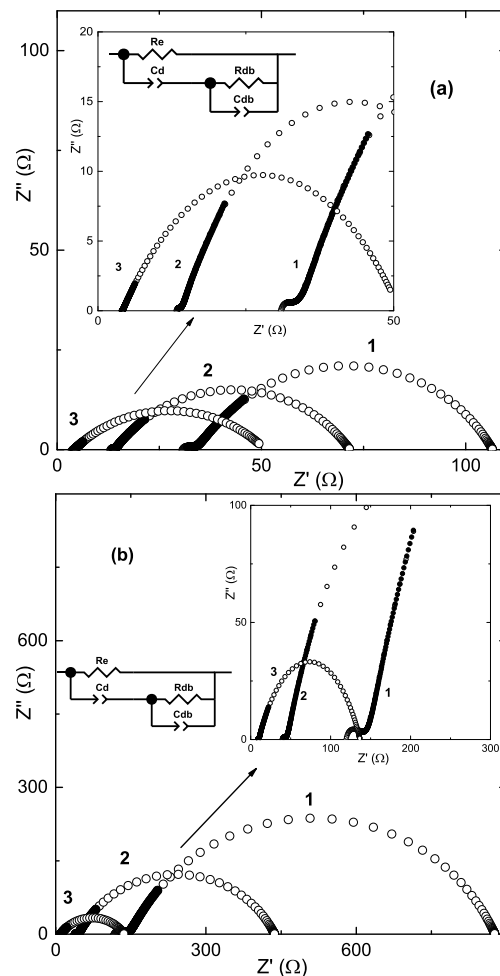


**Fig. 3.** Nyquist plots for  $(\text{Cu}_{0.75}\text{Ag}_{0.25})_7\text{GeS}_5\text{I}$  (a) and  $(\text{Cu}_{0.5}\text{Ag}_{0.5})_7\text{GeS}_5\text{I}$  (b) mixed crystals at 298 K (1), 323 K (2) and 338 K (3): experimental data (solid symbols), modeled (calculated) data (open symbols), and EEC

to  $\text{Ag}_7\text{GeS}_5\text{I}$  crystal leads to the complication of EEC selected for the description of experimental results (Fig. 4).

This is associated with a significant decrease in the electronic component of the conductivity, since, for  $(\text{Cu}_{0.25}\text{Ag}_{0.75})_7\text{GeS}_5\text{I}$  mixed crystal,  $\sigma_{\text{ion}} > \sigma_{\text{el}}$ , and, for  $\text{Ag}_7\text{GeS}_5\text{I}$  crystal,  $\sigma_{\text{ion}} \gg \sigma_{\text{el}}$ . In this regard, the electronic component of the conductivity was determined only in the temperature range of 313–383 K. As can be seen from Fig. 4, low-frequency semicircles are further displaced into the low-frequency region, which is the evidence that the influence of the diffusion and relaxation ionic pro-

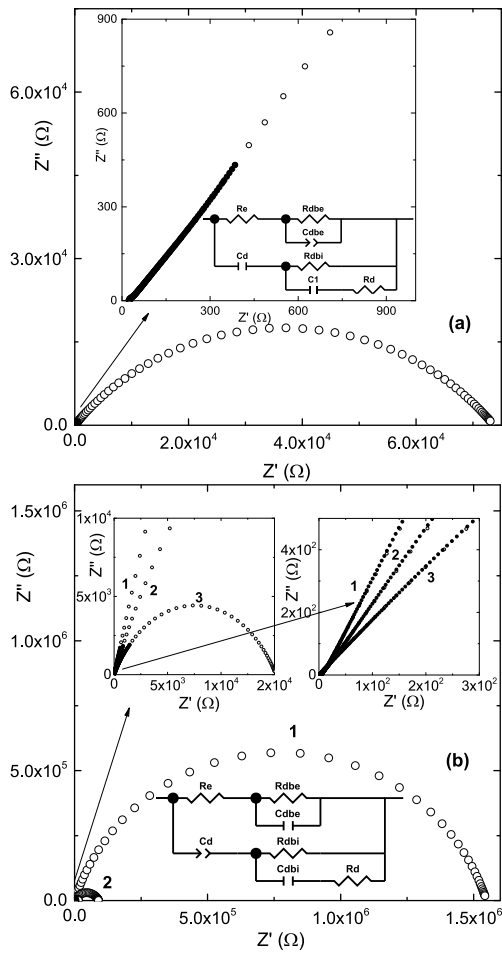


**Fig. 4.** Nyquist plots for  $(\text{Cu}_{0.25}\text{Ag}_{0.75})_7\text{GeS}_5\text{I}$  (a) mixed crystal at 323 K and  $\text{Ag}_7\text{GeS}_5\text{I}$  (b) crystal at 313 K (1), 343 K (2) and 373 K (3): experimental data (solid symbols), modeled (calculated) data (open symbols), and EEC

cesses dominates. This, in turn, leads to a fuzzy representation of high-frequency semicircles. Thus, the low-frequency semicircles in the Nyquist plots correspond to the capacity of the double diffusion layer  $C_d$  with parallelly included electronic resistance  $R_e$ . Due to the decrease of the electronic component of the conductivity, EEC is complicated by the presence of the electronic resistance of domain boundaries  $R_{dbe}$  with parallelly included capacity  $C_{dbe}$ . High-frequency semicircles, in turn, can be described by the ionic resistance of domain boundaries  $R_{dbi}$  with parallelly included  $R_d C_{dbi}$ , which are determining for the ionic resistance of domains and the capacity of domain boundaries. Additionally, parallel to

them, the electronic processes, which are described earlier, occur. As a result, the ionic conductivity is determined by the sum of the resistances  $R_{dbi}$  and  $R_d$ , and the electronic conductivity is determined by  $R_e$  and  $R_{dbe}$ , respectively. The temperature studies have shown that with temperature increasing, the increase of the electronic conductivity gradually eliminates the influence of diffusion ionic processes at the boundaries of crystal domains, as evidenced by the decrease of the high-frequency semicircle at 323 K (Figs. 3 and 4, curve 2). With a further increase of the temperature up to 373 K (Figs. 3 and 4, curve 3), there is a further reduction of the influence of diffusion ionic processes, which, together with the decrease in the thickness of the double diffusion layer, eventually leads to the complete disappearance of the high-frequency semicircle. The analysis of impedance spectra made it possible to investigate the temperature and compositional behavior of the ionic and electronic components of the conductivity of  $(\text{Cu}_{1-x}\text{Ag}_x)_7\text{GeS}_5\text{I}$  mixed crystals. It was established that the compositional dependence of the ionic conductivity is nonmonotonous and nonlinear (Fig. 5, a), which is reflected in the presence of a minimum of the conductivity for  $(\text{Cu}_{0.25}\text{Ag}_{0.75})_7\text{GeS}_5\text{I}$  mixed crystal ( $5.43 \times 10^{-5}$  S/cm), whereas the ionic component of the conductivity for  $\text{Cu}_7\text{GeS}_5\text{I}$  crystal at 298 K is  $6.85 \times 10^{-3}$  S/cm, which is comparable with the corresponding value for  $\text{Ag}_7\text{GeS}_5\text{I}$  crystal ( $7.98 \times 10^{-3}$  S/cm). This is caused by the growth of maximal distances between the moving positions of  $\text{Cu}^+(\text{Ag}^+)$  in the conductivity “net” [7], which is one of the limiting factors of the migration of cations in the crystal (Fig. 5, a). Instead, the electronic conductivity value, which, for  $\text{Cu}_7\text{GeS}_5\text{I}$  crystal, constitutes  $7.35 \times 10^{-2}$  S/cm, in the process of cationic  $\text{Cu}^+ \leftrightarrow \text{Ag}^+$  substitution decreases monotonously and, for  $\text{Ag}_7\text{GeS}_5\text{I}$  crystal, is  $\sim 6.86 \times 10^{-8}$  S/cm (Fig. 5, b).

Since one of the main characteristics of superionic materials is the ratio of the ionic conductivity to the electronic one, we show, in Fig. 5, b, its concentration dependence. It was found that, in the process of cationic  $\text{Cu}^+ \leftrightarrow \text{Ag}^+$  substitution during the transition from the  $\text{Cu}_7\text{GeS}_5\text{I}$  crystal, for which the electronic conductivity is 10 times higher than the ionic one to the  $\text{Ag}_7\text{GeS}_5\text{I}$  crystal, the ratio  $\sigma_{\text{ion}}/\sigma_{\text{el}}$  tends to a monotonous growth, and, for  $\text{Ag}_7\text{GeS}_5\text{I}$  crystal, the ionic conductivity is more than  $10^6$  times greater than the electronic conductivity. Figure 6 shows the tem-

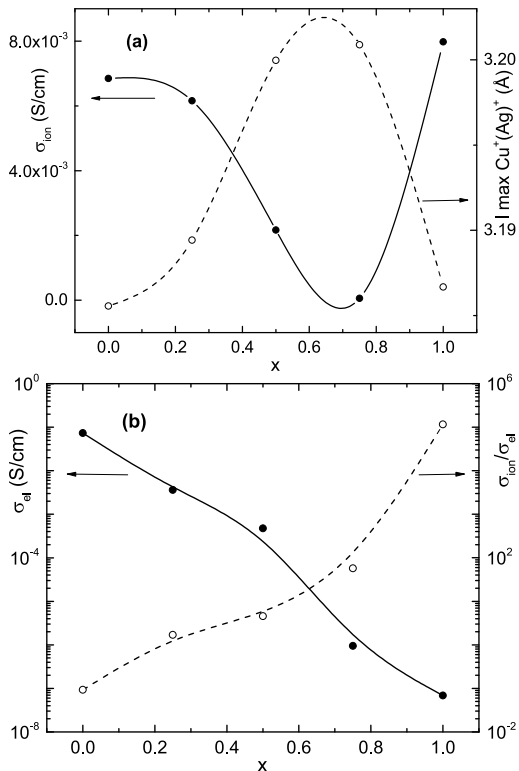


**Fig. 5.** Compositional dependences of the ionic conductivity and maximal distance between the moving positions of  $\text{Cu}^+(\text{Ag}^+)$  in the conductivity “net” for  $(\text{Cu}_{1-x}\text{Ag}_x)_7\text{GeS}_5\text{I}$  mixed crystals at  $T = 298\text{ K}$  (a). Compositional dependences of the electronic conductivity and the ratio  $\sigma_{\text{ion}}/\sigma_{\text{el}}$  for  $(\text{Cu}_{1-x}\text{Ag}_x)_7\text{GeS}_5\text{I}$  mixed crystals at  $T = 298\text{ K}$  (b)

perature dependences of the ionic and electronic components of the conductivity in the Arrhenius coordinates. It is established that they are linear and are described by the Arrhenius law, which confirms the thermoactivating character of the electrical conductivity. With their help, the activation energies were determined, both for the ionic and for the electronic components of the conductivity (Fig. 7).

On the compositional dependence of the activation energy of the ionic conductivity, a nonlinear growth was revealed, which reaches a maximum of 0.768 eV for  $(\text{Cu}_{0.25}\text{Ag}_{0.75})_7\text{GeS}_5\text{I}$  mixed crystal. A growth of the activation energy of the ionic conductivity in mixed crystals compared to  $\text{Cu}_7\text{GeS}_5\text{I}$  crystal ( $E_{a(\text{ion})} = 0.175\text{ eV}$ ) and  $\text{Ag}_7\text{GeS}_5\text{I}$  crystal ( $E_{a(\text{ion})} = 0.258\text{ eV}$ ) is associated with increasing influence of the compositional disordering, namely reducing the mobility of positions  $\text{Cu}^+(\text{Ag}^+)$ , as indicated by the

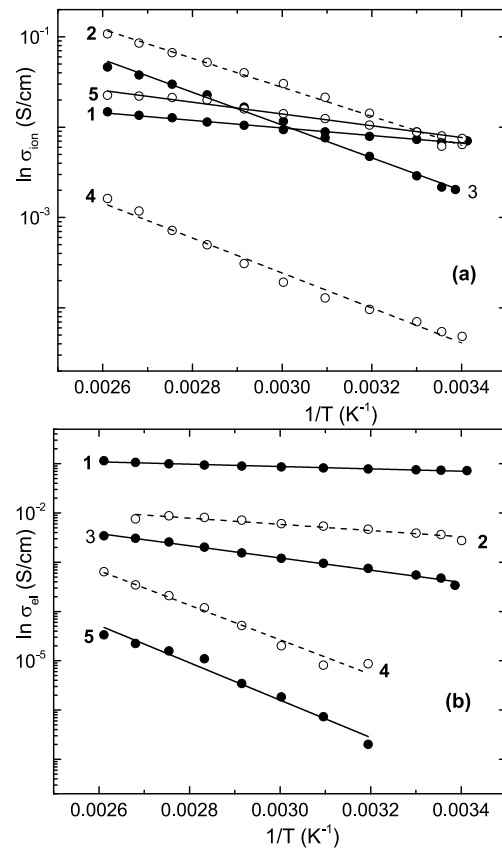


**Fig. 6.** Temperature dependences of the ionic (a) and electronic (b) conductivities for  $(\text{Cu}_{1-x}\text{Ag}_x)_7\text{GeS}_5\text{I}$  mixed crystals:  $\text{Cu}_7\text{GeS}_5\text{I}$  (1),  $(\text{Cu}_{0.75}\text{Ag}_{0.25})_7\text{GeS}_5\text{I}$  (2),  $(\text{Cu}_{0.5}\text{Ag}_{0.5})_7\text{GeS}_5\text{I}$  (3),  $(\text{Cu}_{0.25}\text{Ag}_{0.75})_7\text{GeS}_5\text{I}$  (4), and  $\text{Ag}_7\text{GeS}_5\text{I}$  (5)

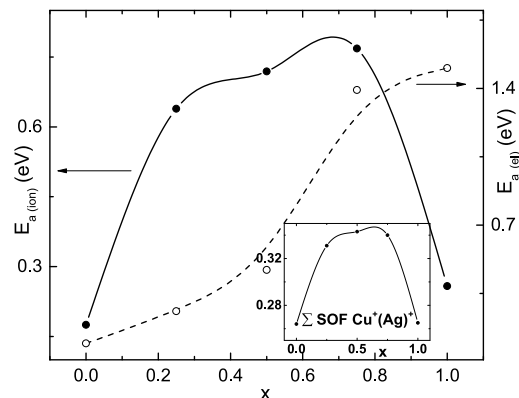


**Fig. 7.** Compositional dependences of the activation energy of the ionic and electronic components of the conductivity for  $(\text{Cu}_{1-x}\text{Ag}_x)_7\text{GeS}_5\text{I}$  mixed crystals. The inset shows the compositional dependence of SOF for the movable atom positions in the crystal lattice

growth of the site occupancy factor (SOF) (Fig. 7, c) [7], which hinders the process of ionic transport. At the same time, the activation energy of the electronic conductivity also increases nonlinearly during the transition from  $\text{Cu}_7\text{GeS}_5\text{I}$  crystal ( $E_{a(\text{el})} = 0.094$  eV) to  $\text{Ag}_7\text{GeS}_5\text{I}$  crystal ( $E_{a(\text{el})} = 1.505$  eV), although without visible features (Fig. 7).

#### 4. Conclusions

The vertical zone crystallization method was employed for the growth of  $(\text{Cu}_{1-x}\text{Ag}_x)_7\text{GeS}_5\text{I}$  mixed crystals, which belong to the cubic syngony F-43m. The frequency and temperature impedance studies were performed in the frequency range from 10 Hz to 300 kHz and in the temperature interval from 292 K to 383 K. The ionic and electronic components of the total electrical conductivity were determined from the Nyquist plots due to the constructed electrode equivalent circuits. The carried out temperature studies allowed to calculate the values of the activation energies of ionic and electronic conductivities. With the help of compositional dependences, it is established that, under  $\text{Cu} \rightarrow \text{Ag}$  cation substitution, the ionic conductivity in  $(\text{Cu}_{1-x}\text{Ag}_x)_7\text{GeS}_5\text{I}$  mixed crystals nonlinearly changes with a minimum at  $x = 0.75$ , whereas the electronic conductivity decreases monotonously. It should be noted that the activation energy of ionic conductivity under  $\text{Cu} \rightarrow \text{Ag}$  cationic substitution, on the contrary, changes nonlinearly with a maximum at  $x=0.75$ , and the activation energy of electronic conductivity increases nonlinearly without any features. The anomalous behavior of the ionic conductivity and its activation energy are associated with the influence of the compositional disordering and the peculiarities of the structural reorganization of the cationic sublattice in  $(\text{Cu}_{1-x}\text{Ag}_x)_7\text{GeS}_5\text{I}$  mixed crystals. Finally, it is established that, with an increase in the content of Ag atoms in  $(\text{Cu}_{1-x}\text{Ag}_x)_7\text{GeS}_5\text{I}$  mixed crystals, the ratio of the ionic conductivity to the electronic one  $\sigma_{\text{ion}}/\sigma_{\text{el}}$  increases, and, for  $\text{Ag}_7\text{GeS}_5\text{I}$  crystal, the ionic conductivity is more than  $10^6$  times greater than the electronic conductivity. This opens up promising ways for the use of  $\text{Ag}_7\text{GeS}_5\text{I}$  crystals as high-performance solid electrolytes.

1. I. Garagounis, V. Kyriakou, C. Anagnostou, V. Bourganis, I. Papachristou, M. Stoukides. Solid electrolytes: Applications in heterogeneous catalysis and chemical cogeneration. *Industr. & Engin. Chem. Res.* **50**, 431 (2011).

2. J.B. Goodenough, P. Singh. Review – solid electrolytes in rechargeable electrochemical cells. *J. Electrochem. Soc.* **162**, A2387 (2015).
3. F. Zheng, M. Kotobuki, S. Song, M.O. Lai, L. Lu. Review on solid electrolytes for all-solid-state lithium-ion batteries. *J. Power Sources* **389**, 198 (2018).
4. M. Hou, F. Liang, K. Chen, Y. Dai, D. Xue. Challenges and perspectives of NASICON-type solid electrolytes for all-solid-state lithium batteries. *Nanotechnology* **31**, 132003 (2020).
5. W.F. Kuhs, R. Nitsche, K. Scheunemann. The argyrodites – a new family of the tetrahedrally close-packed structures. *Mater. Res. Bull.* **14**, 241 (1979).
6. T. Nilges, A. Pfitzner. A structural differentiation of quaternary copper argyrodites: Structure-property relations of high temperature ion conductors. *Z. Kristallogr.* **220**, 281 (2005).
7. I.P. Studenyak, M. Kranjčec, M.V. Kurik. Urbach rule and disordering processes in  $\text{Cu}_6\text{P}(\text{S}_{1-x}\text{Se}_x)_5\text{Br}_{1-y}\text{I}_y$  superionic conductors. *J. Phys. Chem. Solids* **67**, 807 (2006).
8. I.P. Studenyak, M. Kranjčec, Gy.S. Kovacs, I.D. Desnica-Frankovic, V.V. Panko, V.Yu. Slivka. The excitonic processes and Urbach rule in  $\text{Cu}_6\text{P}(\text{S}_{1-x}\text{Se}_x)_5\text{I}$  crystals in the sulfur-rich region. *Mat. Res. Bull.* **36**, 123 (2001).
9. I.P. Studenyak, M. Kranjčec, O.A. Mykailo, V.V. Bilanchuk, V.V. Panko, V.V. Tovt. Crystal growth, structural and optical parameters of  $\text{Cu}_6\text{PS}_5(\text{Br}_{1-x}\text{I}_x)$  superionic conductors. *J. Optoelectr. Adv. Mat.* **3**, 879 (2001).
10. A.F. Orliukas, E. Kazakevicius, A. Kezionis, T. Salkus, I.P. Studenyak, R.Yu. Buchuk, I.P. Prits, V.V. Panko. Preparation, electric conductivity and dielectrical properties of  $\text{Cu}_6\text{PS}_5\text{I}$ -based superionic composites. *Solid State Ionics* **180**, 183 (2009).
11. I.P. Studenyak, V.Yu. Izai, V.I. Studenyak, O.V. Kovalchuk, T.M. Kovalchuk, P. Kopčanský, M. Timko, N. Tomašovičová, V. Zavisova, J. Miskuf, I.V. Oleinikova. Influence of  $\text{Cu}_6\text{PS}_5\text{I}$  superionic nanoparticles on the dielectric properties of 6CB liquid crystal. *Liquid Crystals* **44**, 897 (2017).
12. T. Šalkus, E. Kazakevicius, J. Banys, M. Kranjčec, A.A. Chomolyak, Yu.Yu. Neimet, I.P. Studenyak. Influence of grain size effect on electrical properties of  $\text{Cu}_6\text{PS}_5\text{I}$  superionic ceramics. *Solid State Ionics* **262**, 597 (2014).
13. I.P. Studenyak, M.Kranjčec, V.Yu. Izai, A.A. Chomolyak, M. Vorohta, V. Matolin, C. Cserhati, S. Kökényesi. Structural and temperature-related disordering studies of  $\text{Cu}_6\text{PS}_5\text{I}$  amorphous thin films. *Thin Solid Films* **520**, 1729 (2012).
14. S. Boulineau, M. Courty, J.-M. Tarascon, V. Viallet. Mechanochemical synthesis of Li-argyrodite  $\text{Li}_6\text{PS}_5\text{X}$  ( $X = \text{Cl}, \text{Br}, \text{I}$ ) as sulfur-based solid electrolytes for all solid state batteries application. *Solid State Ionics* **221**, 1 (2012).
15. S. Yubuchi, S. Teragawa, K. Aso, K. Tadanaga, A. Hayashi, M. Tatsumisago. Preparation of high lithium-ion conducting  $\text{Li}_6\text{PS}_5\text{Cl}$  solid electrolyte from ethanol solution for

- all-solid-state lithium batteries. *J. Power Sources* **293**, 941 (2015).
16. C. Yu, L. van Eijck, S. Ganapathy, M. Wagemaker. Synthesis, structure and electrochemical performance of the argyrodite  $\text{Li}_6\text{PS}_5\text{Cl}$  solid electrolyte for Li-ion solid state batteries. *Electrochimica Acta* **215**, 93 (2016).
  17. N.C. Rosero-Navarro, T. Kinoshita, A. Miura, M. Higuchi, K. Tadanaga. Effect of the binder content on the electrochemical performance of composite cathode using  $\text{Li}_6\text{PS}_5\text{Cl}$  precursor solution in an all-solid-state lithium battery. *Ionics* **23**, 1619 (2017).
  18. S. Wenzel, S.J. Seldmaier, C. Dietrich, W.G. Zeier, J. Janek. Interfacial reactivity and interphase growth of argyrodite solid electrolytes at lithium metal electrodes. *Solid State Ionics* **318**, 102 (2018).
  19. Z. Zhang, L. Zhang, X. Yan, H. Wang, Y. Liu, C. Yu, X. Cao, L. van Eijck, B. Wen. All-in-one improvement toward  $\text{Li}_6\text{PS}_5\text{Br}$ -based solid electrolytes triggered by compositional tune. *J. Power Sources* **410–411**, 162 (2019).
  20. I.P. Studenyak, A.I. Pogodin, V.I. Studenyak, O.P. Kokhan, Yu.M. Azhniuk, C. Cserhati, S. Kokenyesi, D.R.T. Zahn. Synthesis and characterisation of new potassium-containing argyrodite-type compounds. *Semicond. Phys., Quantum Electron. & Optoelectron.* **22**, 26 (2019).
  21. M. Laqibi, B. Cros, S. Peytavin, M. Ribes. New silver superionic conductors  $\text{Ag}_7\text{XY}_5\text{Z}$  ( $X = \text{Si, Ge, Sn}$ ;  $Y = \text{S, Se}$ ;  $Z = \text{Cl, Br, I}$ ) – synthesis and electrical studies. *Solid State Ionics* **23**, 21 (1987).
  22. I.P. Studenyak, M. Kranjčec, Gy.Sh. Kovacs, I.D. Desnica-Frankovic, A.A. Molnar, V.V. Panko, V.Yu. Slivka. Electrical and optical absorption studies of  $\text{Cu}_7\text{GeS}_5\text{I}$  fast-ion conductor. *J. Phys. Chem. Solids* **63**, 267 (2002).
  23. I.P. Studenyak, M. Kranjčec, V.V. Bilanchuk, O.P. Kokhan, A.F. Orliukas, E. Kazakevicius, A. Kezionis, T. Šalkus. Temperature variation of electrical conductivity and absorption edge in  $\text{Cu}_7\text{GeSe}_5\text{I}$  advanced superionic conductor. *J. Phys. Chem. Solids* **70**, 1478 (2009).
  24. I.P. Studenyak, M. Kranjčec, V.V. Bilanchuk, O.P. Kokhan, A.F. Orliukas, A. Kezionis, E. Kazakevicius, T. Šalkus. Temperature and compositional behavior of electrical conductivity and optical absorption edge in  $\text{Cu}_7\text{Ge}(\text{S}_{1-x}\text{Se}_x)_5\text{I}$  mixed superionic crystals. *Solid State Ionics* **181**, 1596 (2010).
  25. I.P. Studenyak, A.I. Pogodin, O.P. Kokhan, V. Kavaliuke, T. Šalkus, A. Kezionis, A.F. Orliukas. Crystal growth, structural and electrical properties of  $(\text{Cu}_{1-x}\text{Ag}_x)_7\text{GeS}_5\text{I}$  superionic solid solutions. *Solid State Ionics* **329**, 119 (2019).
  26. I.P. Studenyak, A.I. Pogodin, V.I. Studenyak, V.Yu. Izai, M.J. Filep, O.P. Kokhan, M. Kranjčec, P.Kúš. Electrical properties of copper- and silver-containing superionic  $(\text{Cu}_{1-x}\text{Ag}_x)_7\text{SiS}_5\text{I}$  mixed crystals with argyrodite structure. *Solid State Ionics* **345**, 115183 (2020).
  27. A.R. West. *Solid State Chemistry and its Applications Second edition, student edition* (John Wiley & Sons, 2014).
  28. I.P. Studenyak, A.I. Pogodin, M.M. Luchynets, V.I. Studenyak, O.P. Kokhan, P. Kúš. Impedance studies and electrical conductivity of  $(\text{Cu}_{1-x}\text{Ag}_x)_7\text{GeSe}_5\text{I}$  mixed crystals. *J. Alloys and Compounds* **817**, 152792 (2020).
  29. A.K. Ivanov-Schitz, I.V. Murin. *Solid State Ionics* (Univ. Press, 2001) (in Russian).
  30. M.E. Orazem, B. Tribollet. *Electrochemical Impedance Spectroscopy* (John Wiley & Sons, 2008).
  31. R.A. Huggins, Simple method to determine electronic and ionic components of the conductivity in mixed conductors: a review. *Ionics* **8**, 300 (2002).

Received 28.04.20

А.І. Погодін, В.І. Студеняк,  
М.Й. Філеп, О.П. Кокхан, І.П. Студеняк, П. Кус

ВПЛИВ КАТІОННОГО ЗАМІЩЕННЯ  
НА ІОННУ І ЕЛЕКТРОННУ ПРОВІДНІСТЬ  
ТВЕРДИХ РОЗЧИНІВ  $(\text{Cu}_{1-x}\text{Ag}_x)_7\text{GeS}_5\text{I}$

На монокристалічних зразках твердих розчинів  $(\text{Cu}_{1-x}\text{Ag}_x)_7\text{GeS}_5\text{I}$  були проведені імпедансні вимірювання у діапазоні частот від 10 Гц до 300 кГц та в інтервалі температур 292–383 К. Вивчено температурну і частотну залежності електропровідності твердих розчинів  $(\text{Cu}_{1-x}\text{Ag}_x)_7\text{GeS}_5\text{I}$ . На основі аналізу діаграм Найквіста та з використанням електродних еквівалентних схем були встановлені значення іонної та електронної компонент електропровідності. Досліджено концентраційну поведінку іонної та електронної провідності, а також концентраційну поведінку відповідних енергій активацій. Проаналізовано співвідношення іонної та електронної компонент електропровідності для твердих розчинів складу  $(\text{Cu}_{1-x}\text{Ag}_x)_7\text{GeS}_5\text{I}$ .

*Ключові слова:* змішані кристали, електропровідність, діаграма Найквіста, енергія активації, концентраційна залежність.